Electric arc furnace slags in cement-treated materials for road construction: Mechanical and durability properties

Dear Author,

Please, note that changes made to the HTML content will be added to the article before publication, but are not reflected in this PDF.

Note also that this file should not be used for submitting corrections.

JCBM 8011
14 March 2016
ARTICLE IN PRESS
No. of Pages 10, Model 5G

Construction and Building Materials xxx (2016) xxx–xxx

Contents lists available at ScienceDirect

Construction and Building Materials

journal homepage: www.elsevier.com/locate/conbuildmat

Electric arc furnace slags in cement-treated materials for road construction: Mechanical and durability properties

Federico Autelitano, Felice Giuliani *

Dipartimento di Ingegneria Civile, dell'Ambiente, del Territorio e Architettura-DICATeA, University of Parma, Parco Area delle Scienze, 181/A, 43124 Parma, Italy

HIGHLIGHTS

- The aged EAF slags represented suitable aggregates for CTMs.
- Increasing the EAF aggregates content, CTMs developed lower degree of compaction but higher ITS.
- CTMs containing only EAF aggregates showed poor durability performance.
- EAF aggregates partial replacement (30–60%) of natural aggregates produced suitable and durable CTMs.

ARTICLE INFO

Article history:
Received 15 September 2015
Received in revised form 26 February 2016
Accepted 14 March 2016
Available online xxxx

Keywords:
Recycling
Steel slags
EAF aggregates
Road construction
Pavement engineering
Gyratory compactor
Durability

ABSTRACT

Electric arc furnace (EAF) slags are by-products of a widespread steelmaking process. The recycling of these materials as artificial aggregates in different road applications is a well established practice, which has allowed to reduce the consumption of natural resources and to minimize waste production and costs of landfilling. However, these aggregates are still underutilized in cement-treated materials (CTMs), which consist of mixtures of aggregates blended with small amounts of cement and water that harden after compaction to form a strong paving material. In the light of these considerations, different cement-treated materials, each containing different percentages of natural and artificial aggregates were analyzed. After a preliminary characterization of chemical, physical and durability properties of EAF slag aggregates, a mix design procedure based on both moisture-density approach (gyratory compactor) and mechanical testing (unconfined compression test and indirect tensile test) was performed to identify the optimum cement and water content of CTMs. The design mixtures were then subjected to 5 different accelerated aging procedures in order to study the influence of some factors (temperature, pressure and humidity) on the durability of the cement-treated materials. The results highlighted how the EAF slags represent suitable aggregates for cement-treated materials. The use of these aggregates produced a greater compaction difficulty, but guaranteed excellent mechanical performances, above all in terms of indirect tensile strength. The durability analysis demonstrated that the recycled mixtures showed a worse behavior than the reference one, composed only by limestone aggregates. However, if correctly designed, balancing the percentage of natural aggregate replacement, these mixtures could represent suitable and durable solution for base and sub-base pavement layers.

1. Introduction

Italy is the second country in Europe, after Germany, for the production of steel, with 23.7 million tons in 2014. With regard to the process, the production of electric arc furnace (EAF), which recycles mainly steel scraps, accounts for about 72.5% of the total (17.2 million tons). In this steel-making process about 150 kg of EAF slag per ton of steel are produced, leading to a total amount of more than 2.5 million tons every year [1]. The recycling of steel slags, as artificial aggregates, in concrete and cement industry or in road and geotechnical applications has progressively increased in recent years both in Italy and in all industrially-developed countries. This practice promotes a model of sustainable development, based on reducing the consumption of natural resources and on minimizing waste production and costs of landfilling [2–4].

In comparison to other recyclable materials, such as fly ash, bottom-ash, tire shreds, cement kiln dust or foundry sand, steel slags are underutilized [5]. In fact, many countries have limits and allowances on the use of EAF aggregates, due to their chemical

* Corresponding author.
E-mail address: felice.giuliani@unipr.it (F. Giuliani).

http://dx.doi.org/10.1016/j.conbuildmat.2016.03.054
0950-0618/© 2016 Published by Elsevier Ltd.

Please cite this article in press as: F. Autelitano, F. Giuliani, Electric arc furnace slags in cement-treated materials for road construction: Mechanical and durability properties, Constr. Build. Mater. (2016), http://dx.doi.org/10.1016/j.conbuildmat.2016.03.054

composition. The presence of free expansive compound (CaO, MgO) in EAF slags mineralogy can have a deleterious impact on pavement volume stability, producing upheaval, swelling and accelerated deterioration [2,6,7]. In presence of water, free lime forms portlandite ($Ca(OH)_2$) and free magnesium oxide forms periclase ($Mg(OH)_2$), with an increase in solid volumes of about 90–130% for $Ca(OH)_2$ and 120% for $Mg(OH)_2$ [8,9]. In literature there are examples of steel slags stabilization techniques (exposure to weathering, use of additives, water quenching or spaying, high temperature steam treatment) for reducing their volumetric instability. Authors suggested a minimum aging period of 4–6 months to transform these expansive components into stable forms [6,7,10]. Moreover, the possible leaching of heavy-metals (Pb, Zn, Cu, As, Sb, Cd) can cause soil and groundwater pollution [11]. Studies were recently conducted to solve this environmental problem. Different laboratory treatments were developed to transform EAF slags into environmental friendly materials, characterized by very low hazardous polluting elements content [12].

With reference to road construction, EAF aggregates were successfully used due to their excellent mechanical characteristics. Some authors demonstrated satisfactory applications of EAF slags in non-structural pavement surface treatments using hot mix asphalt (HMA) mixtures [13–15] and warm mix asphalt (WMA) mixtures [16]. Others underlined also the outstanding performances exhibited by steel aggregates in road bases and subbases both in bound and unbound layers [17–19]. Nevertheless, EAF aggregates have seen relatively few road applications in cement bound mixtures, above all in cement-treated layers [20].

Generally, cement-treated material (CTM) consists of an intimate mixture of graded natural or crushed aggregates blended with measured amounts of cement (2%–4%) and water (4%–7%) that hardens after compaction to form a strong paving material [21,22]. The CTM needs proper mix design, adequate thickness, and diligent construction in order to obtain suitable fatigue strength and stiffness, which do not lead to shrinkage and thus cracking in the surface paving. A suitable stiffness of CTM can improve the fatigue resistance and reduce deflection, rutting and other asphalt strains, but can also avoid the sharp step of rigidity between the concrete slab and the subgrade [23]. Moreover, it represents a durable solution, because it is resistant to freeze-thaw and wetting-drying deterioration. Depending on project needs, CTM increases the construction speed, enhances the structural capacity of the pavement, or in some cases reduces the overall time project [24].

The physical and mechanical performances of CTM and the thickness of the layer are strongly affected by several factors, such as cement content, compaction characteristics, aggregate gradation and the quality of aggregates [25]. Too little cement can cause problems of homogenization of the mixture and provides insufficient structural capacity, allowing excessive pavement deflections under heavy traffic loading. Over-rich cement layers, besides being too expensive, are instead too stiff and prone to shrinkage cracking, causing accelerated pavement failure [24,26,27].

The requirements for CTM in different countries are generally expressed in terms of unconfined compressive strength (UCS) at 7-days curing time (Table 1) [25,27–29]. The required values strongly depend on the road class and material type relies heavily on the required UCS. The international requirements for CTMs suggest that the unconfined compressive strength test is performed on specimens compacted with Modified Proctor procedure (EN 13286-2: 2010), whereas Italian specification considers also the gyratory compaction (EN 12697-31:2007). The compressive strength, which depends on several factors (degree of compaction, shape of the specimen, curing time and condition), is a representative parameter of stability and stiffness of the cement-treated layer. However, especially for the cement-treated base beneath a bituminous pavement, the assessment of the mixture's fatigue behavior is more important and significant. Therefore, some countries, besides the UCS performance, recommend limits on the indirect tensile strength (ITS), in order to evaluate the fatigue strength of CTMs.

Table 1
Requirements (technical specifications) for CTMs in different countries.

Country	Cement content (%)	Requirement	
		UCS at 7-days curing time (MPa)	
Australia	3–8	>3	
Brazil	∼4	>3.5	
China	>4% (Road-mix method) >5% (Central-plant mixing)	>2 (Base) >4 (Subbase)	
Spain	3.5–6%	4.5–6	
UK	2–5%	2.5–4.5 (CM1) 4.5–7.5 (CM2)	
USA	3–10%	3.5–6.9 (under PCC) 5.2–6.9 (under HMA)	
		UCS at 7-days (MPa)	ITS at 7-days (MPa)
Italy	2–4%	2.5–5.5 (Gyratory compactor) 2.5–4.5 (Proctor hammer)	0.32–0.60 (Gyratory compactor) >0.25 (Proctor hammer)
South Africa	1.5–3%	1.5–3.0	>0.25
	3–5%	0.75–1.5	>0.20
		UCS at 90-days (MPa)	TS* at 90-days (MPa)
France	2.5–4%	5–10	1

* TS = Tensile strength.

Cement-treated materials containing EAF aggregates, as complete or partial replacement of natural aggregates, exhibits elastic compressive and tensile strength values comparable or better than those of the natural CTMs. Moreover, these recycled mixtures represents economical base pavements, besides being a sustainable paving option, allowing a decreasing in layer thickness [20,30–31].

With regards to the durability of these mixtures, there are no references in literature. Few studies provided the evaluation of both mechanical properties and durability only on concrete containing EAF slag. Some of these studies have shown acceptable durability of concrete with EAF, thought slightly lower than the conventional concrete, despite rather aggressive test conditions and accelerated aging procedures (freezing and thawing cycles, wetting and drying cycles, swelling procedures, climatic chamber and high pressure aging) [32–36].

This experimental study planned to investigate the chemical and mineralogical composition, the concentration of pollutants and the physico-mechanical properties of EAF aggregates. Additionally, several cement-treated materials containing different replacements of EAF aggregates were prepared to characterize their mechanical and durability performances.

2. Materials and methods

2.1. Testing program

The testing program was divided in three main phases. The first step consisted in a preliminary characterization of chemical, physical and durability properties of EAF slag aggregates, following the requirements of EN 13242:2008 and the toxic characteristic leachability according to EN 12457-2:2007. Secondly a mix design procedure based on both moisture-density approach (gyratory compactor) and mechanical testing (unconfined compression test and indirect tensile test) was performed to identify the optimum cement and water content of CTMs. Finally, the design mixtures, characterized by the optimum cement and water content, were subjected to a detailed study about the influence of some factors (temperature, pressure and humidity) on the durability of the CTMs.

Table 2
Oxide composition and heavy metal content of aged EAF aggregates.

	EAF 0/20 mm	EAF 14/32 mm
	Value	
Oxide		
Calcium oxide (CaO) (%)	18.28	16.46
Silicon dioxide (SiO_2) (%)	18.90	19.10
Aluminum oxide (Al_2O_3) (%)	5.80	5.84
Magnesium oxide (MgO) (%)	2.53	2.02
Iron oxide (FeO) (%)	37.71	39.75
Manganese (II) oxide (MnO) (%)	2.55	2.78
Titanium dioxide (TiO_2) (%)	0.24	0.14
Phosphorus pentoxide (P_2O_5) (%)	0.35	0.51
Element		
Lead (Pb) (mg kg^{-1})	29.3	25.9
Antimony (Sb) (mg kg^{-1})	53.2	59.3
Copper (Cu) (mg kg^{-1})	272.8	323.6
Cadmium (Cd) (mg kg^{-1})	21.7	21.3
Chromium (Cr) (mg kg^{-1})	871.3	933.6
Arsenic (As) (mg kg^{-1})	<0.001	<0.001
Selenium (Se) (mg kg^{-1})	<0.01	<0.01
Mercury (Hg) (mg kg^{-1})	<0.001	<0.001
Zinc (Zn) (mg kg^{-1})	259.7	301.2
Barium (Ba) (mg kg^{-1})	1252.1	1233.7
Beryllium (Be) (mg kg^{-1})	<0.001	<0.001
Cobalt (Co) (mg kg^{-1})	3.7	5.1
Nickel (Ni) (mg kg^{-1})	156.1	105.4
Vanadium (V) (mg kg^{-1})	307.2	368.9
Aluminum (Al) (mg kg^{-1})	30,222.5	29,959.5
Boron (B) (mg kg^{-1})	<0.01	<0.01
Iron (Fe) (mg kg^{-1})	301,466	304,229
Manganese (mg kg^{-1})	32,776	35,361

2.1.1. Phase 1: testing materials and properties

The CTMs selected for the experimental analysis consisted in natural and artificial aggregates, Portland-limestone cement and water. Specifically, two different aggregate types were selected: aged EAF aggregates and limestone aggregates. Portland-limestone cement CEM II/A-LL 42.5R (EN 197-1:2011) was used as hydraulic binder for all the mixtures. The added water was clean and free from detrimental concentrations of acids, alkalis, salts, sugar and other organic or inorganic substances, as required by the regulations (EN 1008:2003).

Steel aggregates were provided by a steel mill operating in northern Italy, whereas crushed limestone aggregates were supplied by a quarry near the steelmaking. EAF aggregates derived from the production of steel bars used for building construction. They were obtained by a separation process (scorification) of the cast steel from impurities present in the electric arc furnace. After the steel slag was slowly cooled, the material was stockpiled for metal recovery and crushed in two suitable grain sizes for road applications (0/20 mm and 14/32 mm). The artificial aggregates underwent an oxidation phase (aging), by exposure to weathering over 6 months, to allow the free lime (CaO) and free magnesium oxide (MgO) to be transformed into stable forms.

The oxide composition and the heavy metal oxide content of aged EAF aggregates were determined using X-ray fluorescence (XRF). Table 2 shows that the major chemical components were CaO, SiO_2, Al_2O_3, MgO, FeO and MnO, which together represent more than the 80% of the total mass.

The mineralogical properties of EAF aggregates were investigated using a X-ray diffraction analysis (XRD). X-ray diffraction was performed using Cu Kα radiation generated from a Cu anode (λ = 1.5418 Å). The scanning angle was in the range of 2θ = 10–80°, where θ represents the X-ray angle of incidence. As already highlighted by Yildirim and Prezzi [6], EAF sample showed a very complex XRD pattern, with several overlapping peaks due to the presence of several crystalline phases in the material. The position, the width and the intensity of each peak, allowed to identify the crystalline phases and to determine the structural properties of the material. The major mineral phases were calcite ($CaCO_3$), dolomite ($CaMg(CO_3)_2$) and wüstite ($Fe_{0.880}O$), while minor phases included larnite (Ca_2SiO_4), magnetite (Fe_3O_4) and quartz (SiO_2).

The EAF aggregate volume stability was determined using two accelerated swelling test methods. Specimens, which were compacted according to modified Proctor procedure (EN 13286-2:2010) or through vibrating table (EN 1744-1:2013), were soaked into hot water (ASTM D4792/D4792M-13) or exposed to steam (EN 1744-1:2013) to accelerate the hydration reactions. Swelling measurements from the steam test satisfied the requirements of group V_5 (maximum expansion < 5%) of EN 13242:2008, whereas the volume expansions, after water-bath swelling test, were clearly smaller compared to the limiting expansion (0.5%) specified in ASTM D2940.

The engineering properties (physico-mechanical properties) of aged EAF and limestone aggregates are reported in Table 3, whereas Table 4 reports the chemical properties of EAF aggregates.

With reference to the geometrical requirements, the EAF aggregates had a polyhedral and angular shape. The excellent toughness, abrasion and polishing resistance, the limited ice sensitivity and the small imbibition coefficient characterized this material. Due to the presence of high iron oxide contents, EAF aggregates had density values (3885–3970 kg m^{-3}) larger than those of natural aggregates, such as limestone (2902 kg m^{-3}).

Toxic characteristic leachability procedure (TCLP) analysis, according to EN 12457-2:2004, was performed on EAF aggregates to assess their leaching properties. Table 5 provides the results of the TCLP analysis compared to the leachate concentration limit values defined by the Italian Ministerial Decree 186/2006.

2.1.2. Phase 2: design mixtures selection

Four different CTMs, each containing different percentages (by volume) of natural and artificial aggregates, were analyzed (Table 6). One mix, which served as reference, was composed entirely of natural limestone aggregates (L). The S mix was prepared only with EAF aggregates, whereas the other two were intermediate limestone/steel slag mixtures (SL and LS). The LS mixture was composed of 30% EAF aggregates (16/31.5 mm) and 70% limestone (0/16 mm), whereas the SL of 60% EAF aggregates (5/31.5 mm) and 40% limestone (0/5 mm). The finest fraction (particle sizes smaller than 0.063 mm) in all the mixtures was represented by limestone filler. The mixtures were combined in accordance to the aggregate grading curve suggested by Italian government-owned road company corporation (ANAS) specifications for CTM (Fig. 1).

Table 4
Chemical properties of EAF steel slag aggregates.

Test	Standard EN	EAF 0/12mm	EAF 14/32mm
		Value	
Water-soluble chloride salts (Mohr method) (% by mass)	EN 1744-1:2013	<0.01	<0.01
Acid soluble sulfates (% by mass)	EN 1744-1:2013	<0.2	<0.2
Total sulfur content (% by mass)	EN 1744-1:2013	<0.1	<0.1
Water soluble-sulfates (% by mass)	EN 1744-1:2013	<0.1	<0.1
Volume expansion (steam test) (%)	EN 1744-1:2013	0.04	0.08
Volume expansion (water bath test) (%)	ASTM D4792/ D4792 M-13	0.03	0.04

Table 3
Physical and durability properties of EAF and limestone aggregates.

Test	Standard EN	EAF 0/12 mm	EAF 14/32 mm	Limestone 0/32 mm
Flakiness index (%)	EN 933-3:2012	8.86	10.67	11.02
Shape index (%)	EN 933-4:2008	6.87	7.62	7.98
Los Angeles coefficient (%)	EN 1097-2:2010	14.14	15.65	22.9
Micro-Deval coefficient (%)	EN 1097-1:2011	7.9	9.1	14.1
Polished stone value (%)	EN 1097-8:2009	56.8	58.9	43.7
Water absorption (%)	EN 1097-6:2013	0.78	0.89	0.51
Freezing and thawing resistance (%)	EN: 1367-1:2007	1.51	2.10	1.21
Sand equivalent test (%)	EN 933-8:2012	81	–	71
Density (kg m^{-3})	EN 1097-6:2013	3970	3885	2902

The initials in () are the category for each parameter described in EN 13242:2008.

Please cite this article in press as: F. Autelitano, F. Giuliani, Electric arc furnace slags in cement-treated materials for road construction: Mechanical and durability properties, Constr. Build. Mater. (2016), http://dx.doi.org/10.1016/j.conbuildmat.2016.03.054

Table 5
Concentrations of pollutants in the leachate (EN 12457-2:2004).

Element	EAF 0/12 mm	EAF 14/32mm	Ministerial Decree 06/186 Limit value
Chlorides (Cl) (mg l^{-1})	3.0	3.0	100
Fluorides (F) (mg l^{-1})	0.1	0.3	1.5
Nitrates (NO_3) (mg l^{-1})	1.1	<1.0	50
Sulfates (SO_4) (mg l^{-1})	3.1	3.2	250
Cyanide (CN) (μg l^{-1})	<5	<10	50
Arsenic (As) (μg l^{-1})	<5	<5	50
Barium (Ba) (mg l^{-1})	0.05	0.20	1
Beryllium (Be) (μg l^{-1})	<1.0	<1.0	10
Cadmium (Cd) (μg l^{-1})	<1.0	<1.0	5
Cobalt (Co) (μg l^{-1})	<5.0	<5.0	250
Chromium (Cr) (μg l^{-1})	34.8	14.6	50
Mercury (Hg) (μg l^{-1})	<1.0	<1.0	1
Nickel (Ni) (μg l^{-1})	<5.0	<5.0	10
Lead (Pb) (μg l^{-1})	<5.0	<5.0	50
Copper (Cu) (mg l^{-1})	<0.01	<0.01	0.05
Selenium (Se) (μg l^{-1})	<5.0	<5.0	10
Vanadium (V) (μg l^{-1})	123.4	65.4	250
Zinc (Zn) (mg l^{-1})	<0.01	<0.01	3
Asbestos (μg l^{-1})	<1.0	<1.0	30
COD (mg l^{-1})	10.0	10.3	30
pH	11.0	7.79	5.5–12.0

Each of the 36 mixtures considered was labelled with the aggregate mix acronym followed by two numbers, separated by slash, which represented the nominal amount of cement and the nominal amount of water.

The cement (c_{nom} (m/m %)) and water (w_{nom} (m/m %)) nominal content varied, at intervals of 1%, between 2–4% and 5–7%, respectively. These values are percentages by mass. The choice to study aggregates with different mineralogical nature and density, required a volumetric approach in the mix design. It was necessary the introduction of α coefficients, defined as the ratio between the density of the natural limestone aggregate (ρ_L) and the mean value of density of each mixture (ρ_M). In this way, the mixtures were prepared using effective cement (c_{eff} (v/v %)) and water (w_{eff} (v/v %)) contents, expressed in volume, obtained multiplying the nominal content (expressed in mass) by the α_M factors (Table 6).

The mix design provided the optimization of water and cement content on the basis of a mix design study conducted by means of gyratory compactor (EN 12697-31:2007). This process permitted to identify the CTM characterized by the highest degree of compaction and workability. Specifically, the compactor ram applied and maintained a vertical pressure of 600 kPa during compaction. The compactor tilted the specimen mold at an angle 1.25° and gyrated it for 180 gyrations at a rate of 30 rpm.

The mix design performed by moisture-density testing was then compared with a mechanical approach. The mechanical properties of the mixtures were evaluated by performing unconfined compressive strength test (EN 13286-41:2006) and indirect tensile strength test (EN 13286-42:2006) on cylindrical specimens prepared with the gyratory compactor, after 7 days (Fig. 2). Specimens were de-molded 24 h after compaction and were cured in air for further 6 days at 23 °C and at 50% relative humidity. Three specimens (diameter = 150 mm; height = 160 mm) were subjected to unconfined compression test and three specimens (diameter = 150 mm; height = 80 mm) were subjected to indirect tensile test. The final

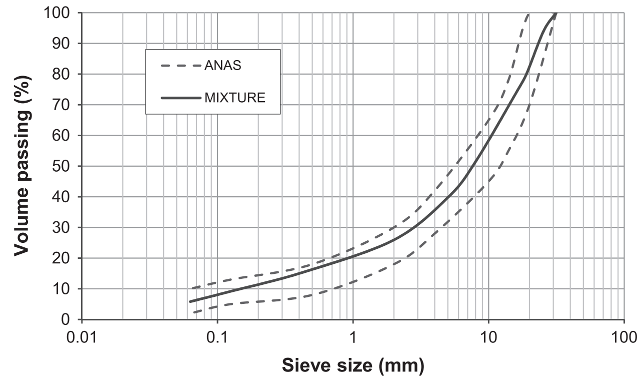

Fig. 1. Volumetric grading curve of the CTMs.

result was then calculated as the mean of the three independent specimens. Then, it was analyzed the evolution of the ITS for different curing times (3, 7, 28 and 50 days).

2.1.3. Phase 3: durability analysis

A detailed study about the influence of several factors on the durability of the CTMs was conducted on the four mixtures characterized by the optimal water and cement content. Three specimens of each mixture, which were cured at 23 °C and at 50% relative humidity for 28 days, were subjected to different conditions of temperature, pressure and humidity, by adopting 5 accelerated aging procedures [34–36]. Before and after each durability test, the tensile strength and the volume were measured. The volume was calculated measuring each dimension of the specimen in three different angular positions (120°) and averaging the results. Therefore, the volume of the specimen was the volume of the minimum circumscribed cylinder. Durability performance was evaluated by comparing the variation of these two parameters and by visual analyzing the samples superficial appearance.

Possible internal damage of CTMs due to own composition was analyzed by means of two different accelerated aging tests, based on swelling procedures, which involved the soaking of specimens into hot water. The objective of these tests was to accelerate hydration reactions of free expansive compounds (CaO and MgO) contained in EAF aggregates and consequently the mixtures swelling behavior.

2.1.3.1. Hot-water bath test. In this test, which was based on the methodology proposed in the ASTM D4792/D4792M-13 standard, the specimens were stored in a hot-water bath maintained at 70 °C for 20 days. Each specimen was then removed from the bath, surface dried and slow cooled at 25 °C for 2 h.

2.1.3.2. High pressure test. The specimens were placed in a pressure pot and soaked in water at temperature of 112 °C and at a pressure of 155 kPa (1.55 bar) for 3 h. In order to assure that both surfaces of each specimen had free access to water, a stainless steel mesh with adjustable leveling feet was placed at the bottom of the pressure pot.

In parallel 3 cyclic procedures, which caused continuous moisture movement through mixtures pores, in order to simulate a possible environmental degradation, were performed.

Table 6
Aggregate type and composition of the mixtures.

Mixture	EAF (m/m %)	Limestone (m/m %)	ρ_M (kg m^{-3})	$\alpha_M = \frac{\rho_L}{\rho_M}$	c_{nom} (m/m %)	c_{eff} (v/v %)	w_{nom} (m/m %)	w_{eff} (v/v %)
L	0	100	2753	1.000	2	2	5	5
					3	3	6	6
					4	4	7	7
LS	30	70	3141	0.877	2	1.8	5	4.4
					3	2.6	6	5.3
					4	3.5	7	6.1
SL	60	40	3518	0.783	2	1.6	5	3.9
					3	2.4	6	4.7
					4	3.1	7	5.5
S	94	6	3824	0.720	2	1.4	5	3.6
					3	2.2	6	4.3
					4	2.9	7	5.0

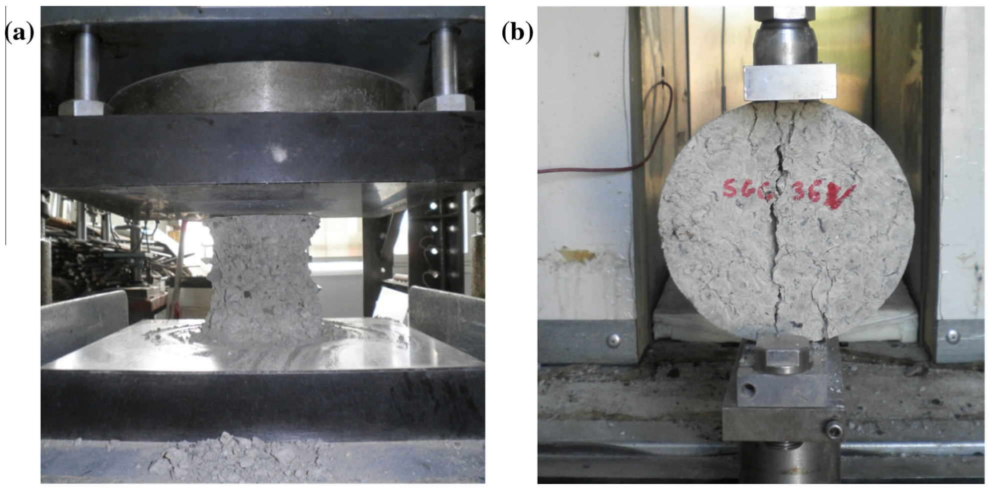

Fig. 2. Unconfined compressive strength test (a) and indirect tensile strength test (b).

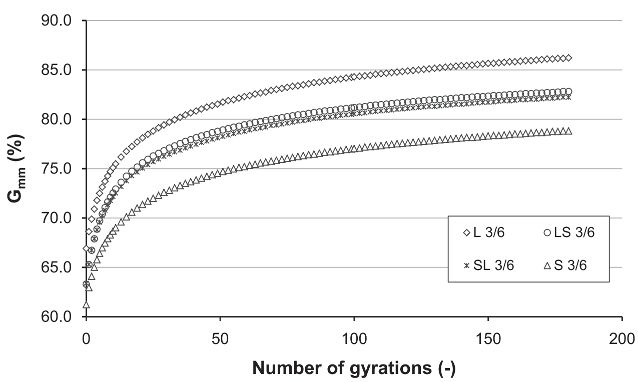

Fig. 3. Densification curves for the optimum mixtures.

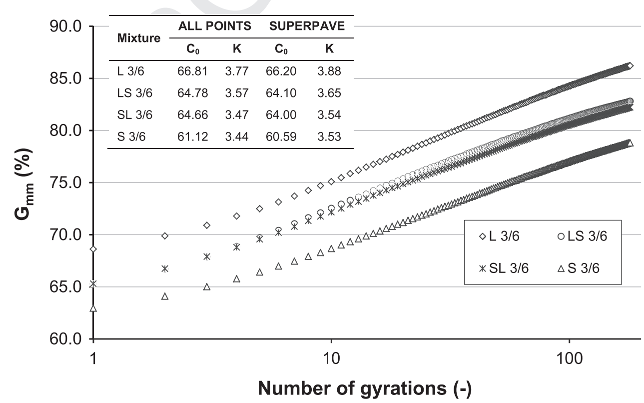

Fig. 4. Densification curves for the optimum mixtures in a semi-logarithmic scale.

2.1.3.3. Freezing and thawing cycles. The specimens were subjected to 20 daily cycles of freezing and thawing; they were maintained at −19 °C for 18 h and at 4 °C for 6 h in a climate chamber. Before the test, the specimen were fully saturated with water through a membrane vacuum pump and subsequently stored in watertight plastic bags to avoid the evaporation of the water.

2.1.3.4. Wetting and drying cycles. In order to study the combined effect of temperature and moisture, the samples were subjected to 20 daily cycles of wetting, through immersion in water at 23 °C for 16 h, and oven drying at 110 °C for 8 h.

2.1.3.5. Thermal shock test. This test planned two cycles of water immersion in the pressure pot at temperature of 112 °C and at a pressure of 155 kPa for 3 h, separated by a cycle of freezing at −19 °C for 2 h in a climate chamber, so that the samples underwent thermal shock.

Table 7
Theoretical maximum specific gravity (G_{mm} %) at 180 gyrations of CTMs.

c_{nom} (m/m %)	w_{nom} (m/m %)	Mixture			
		L	LS	SL	S
2	5	84.57	82.32	80.22	75.78
2	6	85.62	82.50	81.28	76.01
2	7	86.86	82.50	83.26	77.78
3	5	83.14	82.08	80.27	76.18
3	6	87.83	83.46	83.77	78.91
3	7	87.19	83.24	82.22	78.75
4	5	85.51	82.40	80.59	77.66
4	6	87.25	83.35	82.01	77.98
4	7	87.63	83.40	83.64	78.83

3. Results and discussion

3.1. Design mixtures selection

Gyratory compaction allowed to describe in depth the degree of compaction of CTMs. During compaction the height of the specimens was automatically measured and both the mixture density and void content were calculated. The test results were plotted in densification curves which describe the bulk specific gravity of

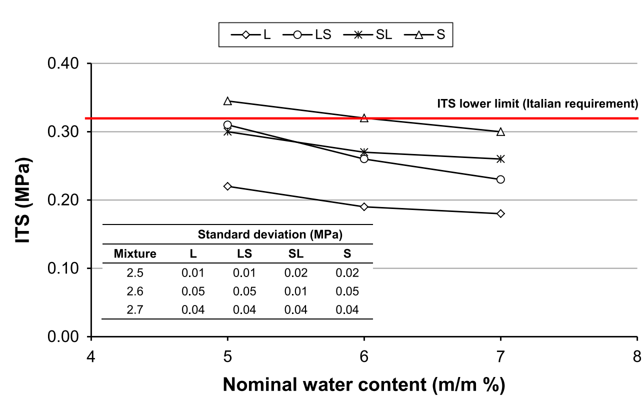

Fig. 5. ITS (with standard deviation) for all mixtures with 2% cement content after 7-days curing time (T = 23 °C and RH = 50%).

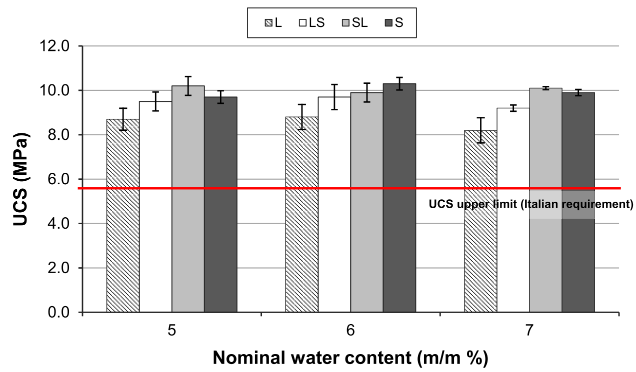

Fig. 6. UCS (with standard deviation) for all mixtures with 4% cement content after 7-days curing time (T = 23 °C and RH = 50%).

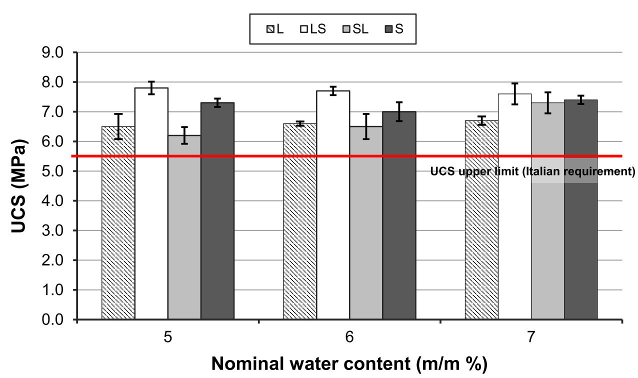

Fig. 7. UCS (with standard deviation) for all mixtures with 3% cement content after 7-days curing time (T = 23 °C and RH = 50%).

the compacted mixture (G_{mb}), expressed in terms of percentage of theoretical maximum specific gravity (G_{mm} %), as a function of number of gyrations.

The optimum densification mixtures were represented, for all mixtures, by the 3% of cement and 6% of water (Table 7 and

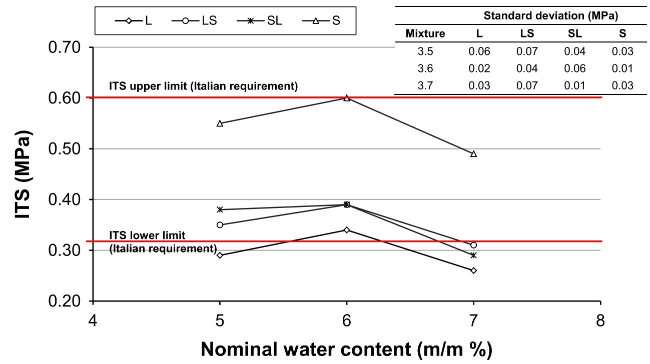

Fig. 8. ITS (with standard deviation) for all mixtures with 3% cement content after 7-days curing time (T = 23 °C and RH = 50%).

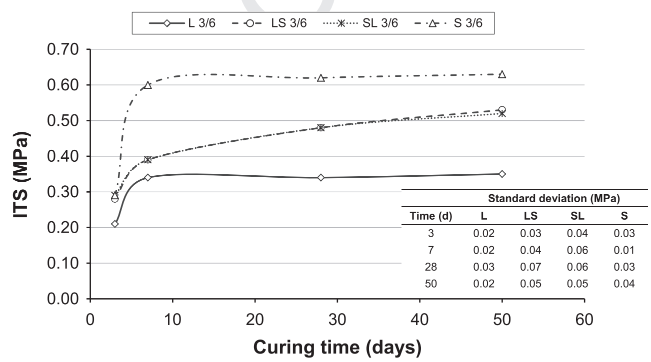

Fig. 9. ITS (with standard deviation) at different curing time (3, 7, 28 and 50 days).

Fig. 3). It can be noted that as the EAF aggregates content increased, the densification curves shift downwards but remained roughly parallel. Therefore the presence of EAF aggregates decreased the level of densification, both during the compaction and in the final stage. The greater compaction difficulty in the mixture containing artificial aggregates can be explained mainly by their surface characteristics. The rough surface texture generates high friction

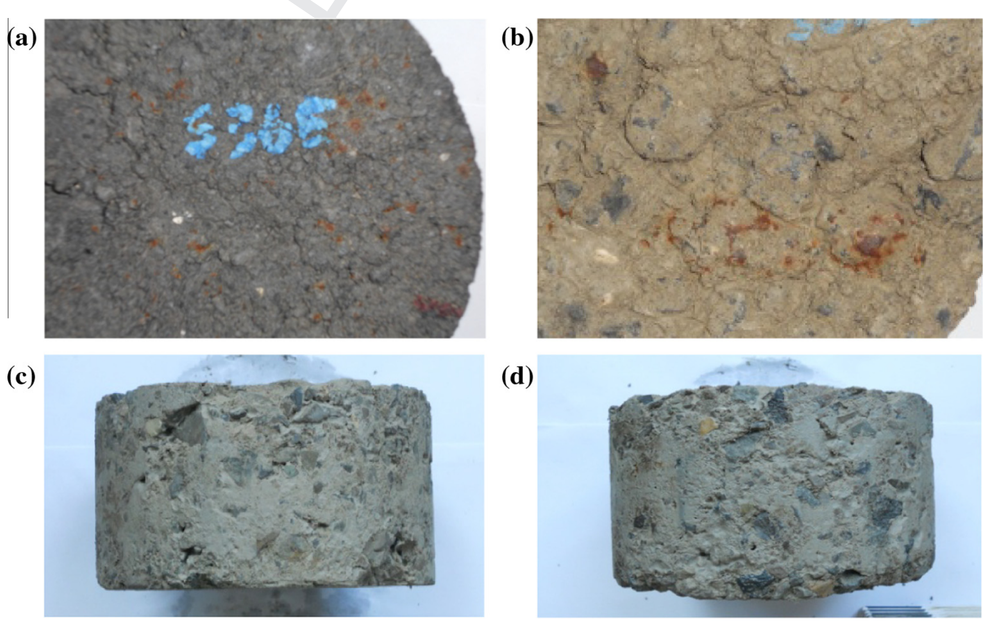

Fig. 10. Superficial appearance of sample representing mixture S (a), SL (b), LS (c) and L (d) after wetting and drying test.

Table 8
Properties of CTM after hot-water bath test.

Mixture	Volume variation (%)	Indirect tensile strength (ITS) (MPa)		Strength variation (%)	Superficial appearance
		Before	After		
L	0.26	0.34	0.45	+32.35	Good
LS	0.24	0.48	0.53	+10.42	Slight oxidization
SL	0.40	0.48	0.50	+4.16	Slight oxidization
					Slight oxidization
S	0.91	0.62	0.37	−40.32	Detachment of coarse aggregates

Table 9
Properties of CTM after high pressure test.

Mixture	Volume variation (%)	Indirect tensile strength (ITS) (MPa)		Strength variation (%)	Superficial appearance
		Before	After		
L	0.40	0.34	0.26	−23.53	Good
LS	0.47	0.48	0.29	−39.58	Good
SL	0.32	0.48	0.31	−35.42	Good
S	0.46	0.62	0.30	−51.61	Slight oxidization

between the particles. For this reason, even for high moisture content (7%), the water was not able to generate a useful lubrication.

By adopting a semi-logarithmic scale, considering the logarithm of the number of gyrations, the densification curves assume a trend which is almost straight. The curves can be represented in a simplified manner following Eq. (1):

$$G_{mm}\,\% = C_0 + K\text{Log}(N) \tag{1}$$

where C_0 defines the degree of self-compaction, that identifies the compaction degree at 0 number of gyrations (vertical shift factor), K is a parameter that represents the workability of the mixture and N is the number of gyrations. According to a linear interpolation, C_0 represents the intercept (at 0 number of gyrations) and K defines the slope and of the regression line which better fits the densification curve. The Superpave (Superior Performing Asphalt Pavements) system, final product of SHRP (Strategic Highway Research Program), suggests to estimate the volumetric properties of the paving mix at three key compaction points: $N_{init} = 8$ (initial number of gyrations), $N_{des} = 100$ (design number of gyrations) and $N_{max} = 180$ (maximum number of gyrations). Specifically, N_{init} corresponds to the state of the mixture as the breakdown roller makes its first few passes, N_{des} describes the anticipated state of density in the mixture after 3–5 years of service (after the indicated amount of traffic) and N_{max} represents the state of density that should never be exceeded in the field [37–38].

The intercept (C_0) and slope (K) constants, describing the regression lines, calculated following both approaches were almost superposed. In terms of workability the behavior of the mixtures was similar and the regression lines were almost parallel: the K values varied from 3.44 (S) to 3.77 (L) considering all the points, whereas varied from 3.53 (S) to 3.88 (L) selecting the 3 key points (N_{init}, N_{des}, N_{max}) suggested by the Superpave criteria (Fig. 4).

The mix design based on the mechanical approach showed that 2% cement content led to unsatisfactory ITS (ITS < 0.32 MPa) (Fig. 5), whereas for 4% cement content the mixtures registered excessive UCS (UCS ≫ 5.5 MPa) (Fig. 6).

Since considering the 3% of cement, the UCS values were slightly higher compared to the Italian requirements (Fig. 7). As can be seen from the Fig. 7, there were no major differences among the mixtures with regards the compressive strengths. Moreover, for equal cement content, the amount of water did not affect significantly the mechanical performances. Otherwise, it could be noted a significant improvement in the tensile strength with increasing the EAF aggregates and a slight reduction with 7% of water content (Fig. 8). The ITS values measured for the L mixture (0.26–0.34 MPa) were half than those of S mixture (0.49–0.60 MPa), while the blended mixes showed an intermediate behavior. The sources of the high increase in tensile strength observed for CTMs containing steel aggregates are probably be attributed to the particle angularity and rough surface texture of EAF aggregates, which contributed

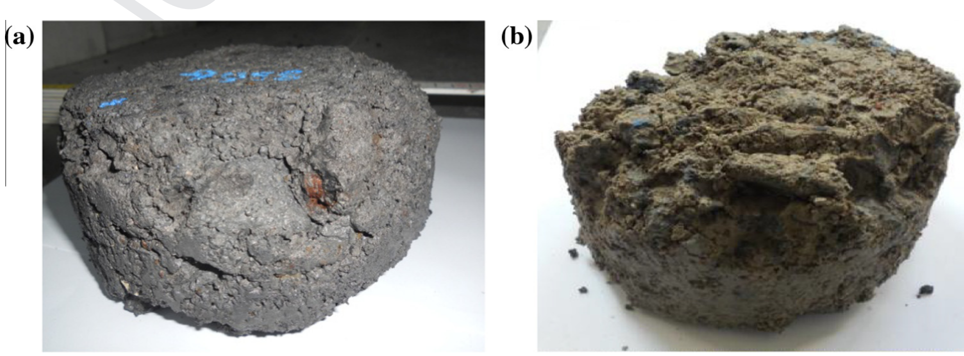

Fig. 11. Internal oxidation of mixture S (a) and disintegration of mixture SL (b).

Please cite this article in press as: F. Autelitano, F. Giuliani, Electric arc furnace slags in cement-treated materials for road construction: Mechanical and durability properties, Constr. Build. Mater. (2016), http://dx.doi.org/10.1016/j.conbuildmat.2016.03.054

Table 10
Properties of CTM after wetting and drying cycles.

Mixture	Volume variation (%)	Indirect tensile strength (ITS) (MPa)		Strength variation (%)	Superficial appearance
		Before	After		
L	0.27	0.34	0.25	−26.47	Stripping Detachment of coarse aggregates
LS	0.35	0.48	0.32	−33.33	Stripping Detachment of coarse aggregates
SL	0.38	0.48	0.26	−45.83	Slight oxidization
S	0.75	0.62	0.32	−48.39	Slight oxidization

Table 11
Properties of CTM after freezing and thawing cycles.

Mixture	Volume variation (%)	Indirect tensile strength (ITS) (MPa)		Strength variation (%)	Superficial appearance
		Before	After		
L	1.07	0.34	0.13	−61.76	Mortar flaking
LS	2.22	0.48	0.13	−72.92	Mortar flaking
SL	n.a*	0.48	n.a*	n.a*	Two specimens almost completely destroyed Significant internal oxidization
S	3.29	0.62	0.14	−77.42	Detachment of coarse aggregates

* Value not available due to the disintegration of the sample.

to create high interparticle friction and particle interlocking, thus to guarantee better tensile strengths.

Therefore the mix design based on the mechanical approach confirmed that the optimum cement and moisture contents were 3% and 6%, respectively.

The curing time is an important factor that affects the mechanical parameters of cement-treated materials. Fig. 9 shows the relationship between ITS and curing time. The graph points out very similar values (0.29 MPa) among the mixtures after 3 days (except for the L mixture), whereas the tensile strengths increased with curing time following different paths for each mix. Specifically, the rate of increase was more rapid during the initial curing period than at later times. The ITS, for the same curing period, increased with increasing steel aggregates content, hence S mixture showed the maximum ITS values.

3.2. Durability analysis

The durability analysis involved 5 different accelerated aging tests, which were performed on three specimens of each mixtures characterized by the optimum cement and water content (c_{nom} = 3% and w_{nom} = 6%).

The hot-water bath test produced slight oxidization and loss of coarse aggregates at the surface in the mixture S; some oxidized parts also occurred in specimens representing mixtures SL and LS. In terms of expansive behavior the effects of immersion in hot water were gradually stronger increasing the percentage of EAF aggregate within the mixtures. The results of mechanical strength after testing highlighted improvements in the order of 5–30% for all mixes, except for the mix S which pointed out a significant fall in ITS (−40.32%) (Table 8).

In the high pressure test, which used the combination of both elevated temperature (hot water) and pressure to accelerate expansive reactions, the final swelling rate confirmed that this testing procedure produced noticeable but homogeneous expansions in all mixtures (about 0.5%). Though the ITS values after test were quite similar for all mixtures (0.26–0.31 MPa), the comparison between the pre-test and post-test values underlined a significant decrease in mechanical performances. Mixture S was more susceptible to loss of strength, having showed ITS negative variations (−51.61%) more than twice as mix L (−23.53%), whereas the blended mixtures exhibited an intermediate behavior (Table 9).

After wetting and drying test, mixture S and SL appeared in good condition, although some specimens showed many signs of oxidation. With regard to mixtures LS and L, the cementitious coating on the natural aggregates was stripped off (especially in the side surface of the specimens), thus the coarse aggregates tended to detach (Fig. 10). This cycling testing accelerated durability problems because it subjected the specimens to the motion and accumulation of harmful materials (sulfates, alkalies, acids, and chlorides) and alternate effects of thermal dilatations and contraction.

The combined effect of wetting and drying caused a slight increase of volume in all mixes (0.27–0.38%), and a more significant value for the mixture S (0.75%). The post-test ITS results identified a reduction in the mechanical performances of all mixtures.

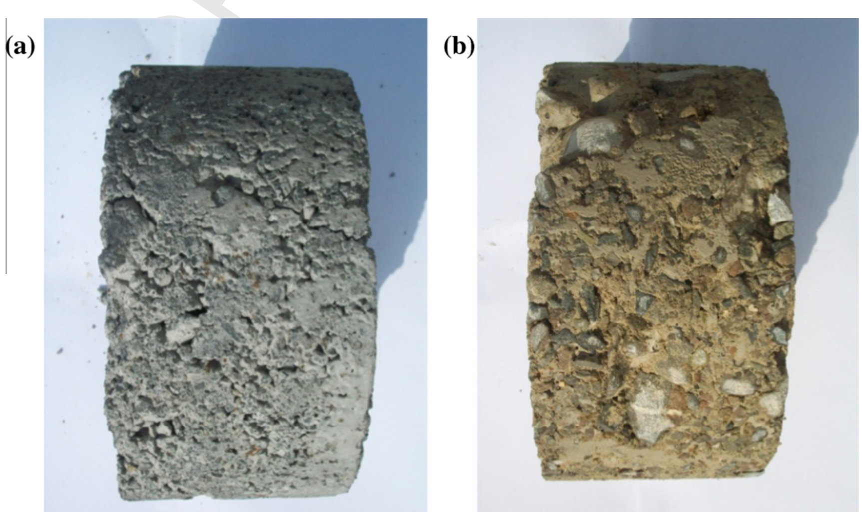

Fig. 12. Superficial appearance of mixture S (a) and stripping in mixture L (b).

Please cite this article in press as: F. Autelitano, F. Giuliani, Electric arc furnace slags in cement-treated materials for road construction: Mechanical and durability properties, Constr. Build. Mater. (2016), http://dx.doi.org/10.1016/j.conbuildmat.2016.03.054

Table 12
Properties of CTM after thermal shock test.

Mixture	Volume variation (%)	Indirect tensile strength (ITS) (MPa)		Strength variation (%)	Superficial appearance
		Before	After		
L	−0.67	0.34	0.21	−38.24	Stripping
LS	0.02	0.48	0.24	−50.00	Stripping
SL	0.38	0.48	0.31	−35.42	Rather good
S	0.62	0.62	0.12	−80.65	Superficial cracking

The trend defined a resistance decrease with the increase in the amount of EAF aggregates. Specifically, mix S (48.39%) pointed out a loss of strength nearly twice than the reference mixture (26.47%) (Table 10).

A considerably severe condition on CTM was the exposure to freezing and thawing cycles. The accumulative effect of successive cycles produced noteworthy volume expansions (1–3%), scaling and superficial spalling. Moreover the test caused sample shape variation and detachment of aggregates, which implied difficulties for a strict evaluation of the volumetric change. When water freezes, it expands about 9% and this movement generates pressures in the pores that, when in excess of the tensile strength of the mixture, cause distress. Specifically, the mixture S showed evident signs of internal oxidation and loss of aggregates even handling the specimens, whereas two specimens of SL mixture were almost completely destroyed (Fig. 11). Although moderately deteriorated, the mixes LS and L were subjected to mortar flaking over coarse aggregate particles (superficial spalling). All mixes showed a significant decrease in strength (60%–70%), in confirmation of a very high severity level of this test. The ITS once again decreased with increasing the content of EAF aggregates within the mixtures (Table 11).

The last durability cycling test was characterized by sudden changes of temperature (thermal shock), either from hot to cold and vice versa. The superficial appearance of the samples was rather good. However, it was observed that in L and LS mixtures many natural aggregates remained uncoated (stripping), as already noted in the wetting and drying test (Fig. 12a). The maintenance of adhesion between the EAF aggregates and the cementitious matrix was probably caused by the rough surface texture of these type of aggregates, characterized by micro-pores. Notwithstanding this, superficial cracks were observed in two specimens of the mixture S, distress almost never detected in this experimental program (Fig. 12b). The existence of the thermal gradient implied difference in thermal expansion of the various parts of the CTMs, causing mixture damage. This procedure caused two opposite volume expansion behaviors: shrinkage in the reference mixture (L) and swelling in mixtures S and SL. Moreover, all mixtures highlighted significant loss of ITS, above all mixture S in which cracks were developed (Table 12).

4. Conclusions

The artificial aggregates, derived from electric arc furnace slags, showed excellent physical and chemical properties in the prequalification phase, representing suitable aggregates for CTMs.

The mix design procedure, based on both moisture-density (gyratory compactor) and mechanical testing (UCS test and ITS test), highlighted that the optimum cement and moisture contents were 3% and 6%, respectively. Lower cement content led to unsatisfactory ITS values, whereas for higher cement content the mixtures registered too high UCS values, compared to the typical international limits. For equal cement content, the amount of water did not affect significantly the UCS, unlike the ITS which slightly decreased with 7% of water content. Moreover, increasing the EAF aggregates replacement, decreased the degree of compaction but increased the indirect tensile strength. The particle angularity and the rough surface texture of EAF aggregates, contributed to create high interparticle friction and particle interlocking in the cementitious matrix. These aspects on the one hand caused a greater compaction difficulty, but on the other hand guaranteed excellent mechanical performances, above all in terms of ITS.

The durability analysis demonstrated that the recycled mixtures showed a worse behavior than the reference one, composed only by limestone aggregates. The CTMs containing only EAF aggregates (mixture S) provided poor quality performances both in terms of swelling, with average volume increase of 1.5%, and of mechanical strengths, with loss of ITS up to 80%. The behavior improved instead for the blended mixtures, composed by natural fine fraction and EAF coarse aggregates. These mixtures registered slight volumetric expansions (about 0.5%) and reductions in mechanical strengths quite close to those measured for the traditional CTM. All mixtures, especially mix S, were extremely susceptible to freezing and thawing cycles, dry and wetting cycles and thermal shock. However, the exposure to large or sharp thermal and moisture excursions are generally less likely to occur, especially at the base and sub-base depth.

In summary, the CTMs containing EAF aggregates need a proper mix design to balance the percentage of natural aggregate replacement. If correctly designed, these mixtures could represent suitable and durable solutions for base and sub-base layers, characterized by excellent performances.

References

[1] B. Federacciai, L'industria siderurgica italiana. Relazione annuale 2014. [The Italian steel industry. Annual Report 2014]. 21st May 2015 Milan, Italy, 2015 (in Italian).
[2] H. Motz, J. Geiseler, Products of steel slags an opportunity to save natural resources, Waste Manage. 21 (3) (2001) 285–293.
[3] T. Zhang, P. Gao, P. Gao, J. Wei, Q. Yu, Effectiveness of novel and traditional methods to incorporate industrial wastes in cementitious materials – an overview, Resour. Conserv. Recycl. 74 (2013) 134–143.
[4] J. de Brito, N. Saikia, Recycled Aggregate in Concrete: Use of Industrial, Construction and Demolition Waste, Springer-Verlag, London, 2013.
[5] A.S. Brand, J.R. Roesler, Concrete With Steel Furnace Slag and Fractionated Reclaimed Asphalt Pavement. Research Report No. ICT-14-015, Illinois Center for Transportation, University of Illinois at Urbana-Champaign, 2014.
[6] I.Z. Yildirim, M. Prezzi, Use of Steel Slag in Subgrade Applications. Publication FHWA/IN/JTRP-2009/32, Joint Transportation Research Program, Indiana Department of Transportation and Purdue University, West Lafayette, Indiana, 2009.
[7] G. Wang, Determination of the expansion force of coarse steel slag aggregate, Constr. Build. Mater. 24 (2010) 1961–1966.
[8] M. Frías Rojas, M.I. Sánchez de Rojas, Chemical assessment of the electric arc furnace slag as construction material: expansive compounds, Cem. Concr. Res. 34 (2004) 1881–1888.
[9] C. Shi, Steel slag - its production, processing and cementitious properties, J. Mater. Civ. Eng. (ASCE) 16 (3) (2004) 230–236.
[10] L.M. Juckes, The volume stability of modern steelmaking slags, Miner. Process. Extr. Metall. Rev. 112 (3) (2003) 177–197.
[11] F. Engström, M. Lidström Larsson, C. Samuelsson, Å. Sandström, R. Robinson, B. Björkman, Leaching behavior of aged steel slags, Steel Res. Int. 85 (4) (2014) 607–615.
[12] Q. Yang, B. Haase, F. Han, F. Engström, J. Li, A. Xu, B. Björkman, Laboratory treatments of EAF slag for its use in construction, Adv. Mater. Res. 726–731 (2013) 2921–2930.
[13] M. Arabani, A.R. Azarhoosh, The effect of recycled concrete aggregate and steel slag on the dynamic properties of asphalt mixtures, Constr. Build. Mater. 35 (2012) 1–7.
[14] A. Bonati, S. Rainieri, G. Bochicchio, B. Tessadri, F. Giuliani, Characterization of thermal properties and combustion behaviour of asphalt mixtures in the cone calorimeter, Fire Saf. J. 74 (2015) 25–31.
[15] A. Kavussi, M.J. Qazizadeh, Fatigue characterization of asphalt mixes containing electric arc furnace (EAF) steel slag subjected to long term aging, Constr. Build. Mater. 72 (2014) 158–166.

[16] M. Ameri, S. Hesami, H.G. Ameri, Laboratory evaluation of warm mix asphalt mixtures containing electric arc furnace (EAF) steel slag, Constr. Build. Mater. 49 (2013) 611–617.

[17] S.A. Aiban, Utilization of steel slag aggregate for road bases, J. Test. Eval. 34 (1) (2006) 65–75.

[18] F. Autelitano, F. Giuliani, Swelling behavior of electric arc furnace aggregates for unbound granular mixtures in road construction, Int. J. Pavement Res. Technol. 8 (2) (2015) 103–111.

[19] D. Shen, C. Wu, J. Du, Laboratory investigation of basic oxygen furnace slag for substitution of aggregate in porous asphalt mixture, Constr. Build. Mater. 23 (2009) 453–461.

[20] M. Pasetto, N. Baldo, Experimental analysis of hydraulically bound mixtures made with waste foundry sand and steel slag, Mater. Struct. 48 (8) (2015) 2489–2503.

[21] A. Grilli, M. Bocci, A.M. Tarantino, Experimental investigation on fibre-reinforced cement-treated materials using reclaimed asphalt, Constr. Build. Mater. 38 (2013) 491–496.

[22] A. Ismail, M. Shojaei Baghini, M.R.B. Karim, F. Shokri, R.A. Al-mansoba, A.A. Firoozi, A.A. Firoozi, Laboratory investigation on the strength characteristics of cement-treated base, Appl. Mech. Mater. 507 (2014) 353–360.

[23] S. Lim, D.G. Zollinger, Estimation of the compressive strength and modulus of elasticity of cement-treated aggregate base materials, Transp. Res. Rec.: J. Transp. Res. Board 1837 (2003) 30–38.

[24] R.L. Varner, Variability of Cement-Treated Layers in MDOT Road Projects. Research Report No. FHWA/MS-DOT-RD-11-227, Mississippi Department of Transportation, Geotechnical and Materials Engineering Consultants, Jackson, Mississippi, 2011.

[25] D.X. Xuan, L.J.M. Houben, A.A.A. Molenaar, Z.H. Shui, Mechanical properties of cement-treated aggregate material – a review, Mater. Des. 33 (2012) 496–502.

[26] W.S. Guthrie, S. Sebesta, T. Scullion, Selecting Optimum Cement Contents for Stabilizing Aggregate Base Materials. Report 4920-2, Texas Transportation Institute, Texas A&M University System, College Station, Texas, 2001.

[27] C. Kraemer, J.M. Pardillo, S. Rocci, M.G. Romana, V.S. Blanco, M.Á. del Val, Ingegnería de carreteras [Road engineering], vol. 2, McGraw-Hill/ Interamericana de España, Aravaca, 2004.

[28] B. Cftr, Applications des nouvelles normes assises de chaussées NF EN 14227 – Mélanges traités aux liants hydrauliques. Spécifications [Application of New Standards for Road Pavement NF EN 14227 – Mixtures Treated With Hydraulic Binders – Specifications]. Note n° 15 – Juillet, 2007 (in French).

[29] M. Shojaei Baghini, A. Ismail, M.R. Karim, F. Shokri, A.A. Firoozi, Effect of styrene-butadiene copolymer latex on properties and durability of road base stabilized with Portland cement additive, Constr. Build. Mater. 68 (15) (2014) 740–749.

[30] L.P. De Bock, H. Van den Bergh, Stainless steel slags in hydraulic bound mixtures for road construction two case studies in Belgium, in: E. Vázquez, C. F. Hendriks, G.M.T. Janssen (Eds.), International RILEM Conference on the Use of Recycled Materials in Buildings and Structures, vol. 2, RILEM Publications, Bagneux, 2004, pp. 1095–1104.

[31] NCHRP, Recycled Materials and Byproducts in Highway Applications, NCHRP Synthesis 435, National Cooperative Highway Research Program, Transportation Research Board, Washington DC, 2013.

[32] G. Adegoloye, A.-L. Beaucour, S. Ortola, A. Noumowé, Concretes made of EAF slag and AOD slag aggregates from stainless steel process: mechanical properties and durability, Constr. Build. Mater. 76 (2015) 313–321.

[33] A.S. Brand, J.R. Roesler, Steel furnace slag aggregate expansion and hardened concrete properties, Cement Concr. Compos. 60 (2015) 1–9.

[34] J.M. Manso, J.A. Polanco, M. Losañez, J.J. Gonzáles, Durability of concrete made with EAF slag as aggregate, Cement Concr. Compos. 28 (2006) 528–534.

[35] C. Pellegrino, V. Gaddo, Mechanical and durability characteristics of concrete containing EAF slag as aggregate, Cement Concr. Compos. 31 (2009) 663–671.

[36] J.A. Polanco, J.M. Manso, J. Setién, J.J. González, Strength and durability of concrete made with electric steelmaking slag, ACI Mater. J. 108 (2) (2011) 196–203.

[37] SHRP, The Superpave Mix Design Manual for New Construction and Overlays, Strategic Highway Research Program National Research Council, Washington, DC, 1994.

[38] NCHRP, Superpave mix design: Verifying gyration levels in the N_{design} table. NCHRP Report 573, National Cooperative Highway Research Program, Transportation Research Board, Washington DC, 2007.

Please cite this article in press as: F. Autelitano, F. Giuliani, Electric arc furnace slags in cement-treated materials for road construction: Mechanical and durability properties, Constr. Build. Mater. (2016), http://dx.doi.org/10.1016/j.conbuildmat.2016.03.054